

Overexpression of Dicer in Precursor Lesions of Lung Adenocarcinoma

Simion Chiosea,¹ Elena Jelezcova,^{2,3} Uma Chandran,⁴ Jianhua Luo,¹
Geeta Mantha,¹ Robert W. Sobol,^{2,3} and Sanja Dacic¹

¹Department of Pathology, University of Pittsburgh Medical Center; ²Department of Pharmacology, University of Pittsburgh School of Medicine; ³University of Pittsburgh Cancer Institute, Hillman Cancer Center; and ⁴Department of Biomedical Informatics, University of Pittsburgh, Pittsburgh, Pennsylvania

Abstract

Differential microRNA (miR) expression is described in non-small cell lung carcinoma. miR biogenesis requires a set of proteins collectively referred to as the miR machinery. In the proposed multistep carcinogenesis model, peripheral adenocarcinoma of the lung develops from noninvasive precursor lesions known as atypical adenomatous hyperplasia (AAH) and bronchioloalveolar carcinoma (BAC). The gene array analysis of BAC and adenocarcinoma showed a transient up-regulation of *Dicer* (a key effector protein for small interfering RNA and miR function) and *PACT* along with down-regulation of most genes encoding miR machinery proteins. Immunohistochemically, *Dicer* was up-regulated in AAH and BAC and down-regulated in areas of invasion and in advanced adenocarcinoma. A fraction of adenocarcinomas lose *Dicer* as a result of deletions at the *Dicer* locus. Expanded immunohistochemical and Western blot analysis showed higher *Dicer* level in squamous cell carcinoma (SCC) of the lung when compared with adenocarcinoma. Other proteins of the RNA-induced silencing complex (RISC; *SND1*, *PACT*, and *FXR1*) were also present at higher levels in a SCC cell line when compared with an adenocarcinoma cell line. In conclusion, the stoichiometry of miR machinery and RISC depends on histologic subtype of lung carcinoma, varies along the AAH-BAC-adenocarcinoma sequence, and might explain the observed abnormal miR profile in lung cancer. The status of the endogenous miR machinery in various histologic subtypes and stages of lung cancer may help to predict the toxicity of and susceptibility to future RNA interference-based therapy. [Cancer Res 2007;67(5):2345–50]

Introduction

Lung cancer is the leading cause of cancer death for both men and women. Recently, adenocarcinoma became the predominant histologic form of lung cancer (1). In the proposed multistep carcinogenesis model, peripheral adenocarcinoma of the lung develops from a precursor lesion referred to as atypical adenomatous hyperplasia (AAH). AAH transforms into nonmucinous bronchioloalveolar carcinoma (BAC), which progresses into invasive adenocarcinoma, just as colon adenomas progress into colon adenocarcinomas (2).

MicroRNAs (miR) are a class of small noncoding 18- to 24-nucleotide-long RNAs that were recently implicated in the development of lung carcinoma: 43 miRs are differentially expressed between lung cancer and benign lung tissue (3).

Production and function of miR require a set of proteins collectively referred to as the miR machinery (summarized in ref. 4). Altered balance of miR machinery proteins can contribute to the development of lung cancer in a miR-guided fashion and independently of the RNA interference (RNAi) pathway. In a miR-guided fashion, the miR machinery regulates the expression of multiple tumor suppressor genes and oncogenes (5). The list of miR with known cancer gene targets continues to grow (e.g., *bcl-2*, *c-myc*, and *RAS*; ref. 6). Independently of the RNAi pathway, *Dicer* controls checkpoints in response to mutagenic stress. *Dicer* has been shown to regulate G₁ arrest in response to nitrogen-limiting conditions and initiate the Cdc2-dependent DNA replication and DNA damage checkpoints (7).

The reduced expression of *Dicer* mRNA in non-small cell lung carcinoma (NSCLC) is associated with shorter postoperative survival (8). In transgenic mice, lungs that lack *Dicer* in the epithelium fail to branch normally and show large, fluid-filled cavities with epithelium being detached from the underlying mesenchyma (9). Another RNA-induced silencing complex (RISC) subunit, *PACT*, is up-regulated in small-sized adenocarcinomas (10). Therefore, it is important to characterize expression of *Dicer* and other endogenous miR machinery proteins in human malignancies.

Using our screening tissue microarray set and NSCLC cell lines, we observed higher levels of several RISC proteins in squamous cell carcinoma (SCC) compared with lung adenocarcinoma. Next, we examined RISC proteins along the AAH-BAC-adenocarcinoma sequence. AAH and BAC are morphologically distinct noninvasive neoplastic lesions. We employed these morphologic entities to study the timing of changes in expression of *Dicer* and other components of the miR machinery in lung adenocarcinoma. Our gene array analysis done on cRNA prepared from manually microdissected formalin-fixed, paraffin-embedded (FFPE) histologic sections showed a dramatic change in expression of most genes encoding proteins of the miR machinery. The up-regulation of *Dicer* in AAH and BAC was confirmed by immunohistochemical analysis of clinical samples. Furthermore, we show decreased level of *Dicer* in invasive lung adenocarcinoma. Finally, a fraction of adenocarcinomas lose *Dicer* as a result of deletions at the *Dicer* locus.

Materials and Methods

Clinical profile of cases and screening paraffin-embedded tissue microarray. Approval for this study was obtained from the Institutional Review Board. Overall, 110 lung tissue specimens were analyzed. The tissue

Requests for reprints: Simion Chiosea, Department of Pathology, University of Pittsburgh Medical Center Presbyterian, C920, 200 Lothrop Street, Pittsburgh, PA 15213. Phone: 412-958-5459; Fax: 412-624-0614; E-mail: chioseasi@upmc.edu.

©2007 American Association for Cancer Research.
doi:10.1158/0008-5472.CAN-06-3533

microarray set consists of 60 lung tissue specimens (9 stage I, 6 stage II, 2 stage III, and 3 stage IV lung adenocarcinoma; 9 SCC; and 31 matched normal lung tissue) from 54 different patients. Each specimen was represented by at least six cores. In addition, full sections of 17 BAC, 11 AAH, and 14 stage I and 8 stage II adenocarcinomas were examined.

Immunohistochemical stains and statistical analysis. Immunohistochemistry was done as previously described (4). Briefly, the slides were incubated at 4°C overnight with anti-Dicer antibodies (Clonogene, Hartford, CT) at 1:600 dilution. The nonneoplastic bronchial epithelium adjacent to the areas of neoplasm served as an internal positive control. We recorded the extent (%) of positive neoplastic cells and intensity of Dicer immunoreactivity in the neoplastic glands for every specimen. The intensity for the AAH, BAC, and adenocarcinomas was graded on a scale from 0 to 3. Dicer staining was scored as "1" if the staining intensity in the neoplasms was lower than the staining intensity of the normal bronchial epithelium. The staining was scored as "2" if the staining intensity in the neoplasm matched the staining intensity of the normal bronchial epithelium. Dicer staining was scored as "3" if the staining intensity in the neoplasms exceeded the staining intensity of the normal bronchial epithelium. Score "0" reflected a lack of Dicer immunoreactivity and was the most common pattern seen in benign alveolar epithelial cells. A composite score was computed for each specimen as the sum of the products between the intensity score and the percentage of tumor with that particular intensity. Histologic sections along the greatest tumor dimension were analyzed. For adenocarcinomas, only the invasive component was scored. Two pathologists (S.D. and S.C.) scored the stained slides. Two sample comparisons were done with the *t* test. All statistical analysis of immunohistochemical studies was done with Sigma Stat (SYSTAT, Point Richmond, CA).

Gene array: cRNA preparation, affymetrix chip hybridization, data preprocessing, and statistical analysis. cRNA was prepared from fifteen 4- μ m-thick FFPE histologic sections of manually microdissected neoplastic and matched benign lung tissue and hybridized to an Affymetrix HGU133 x3p chip as follows. Total RNA was extracted using a MasterPure RNA purification kit (Epicentre Biotechnologies, Waukesha, WI). The extraction process followed the manufacturer's recommendation. Five micrograms of total RNA were used in the first-strand cDNA synthesis with T7-d(T)₂₄ primer [GGCCAGTGAATTGTAATACGACTCACTATAGGGAGGCGG-(dT)₂₄] using Superscript II (Life Technologies, Rockville, MD). The second-strand cDNA synthesis was carried out at 16°C by adding *Escherichia coli* DNA ligase, *E. coli* DNA polymerase I, and RNaseH in the reaction. This was followed by the addition of T4 DNA polymerase to blunt the ends of newly synthesized cDNA. The cDNA was purified through phenol/chloroform and ethanol precipitation. The purified cDNA were then incubated at 37°C for 4 h in an *in vitro* transcription reaction and labeled with biotin using the MEGAscript system (Ambion, Inc., Austin, TX). The cRNA was purified through phenol/chloroform and ethanol precipitation. Reverse transcription was done using random hexamer primers. This is followed by double-stranded cDNA synthesis and cDNA purification as described above. Fifteen to 20 μ g of cRNA were fragmented by incubating in a buffer containing 200 mmol/L Tris-acetate (pH 8.1), 500 mmol/L KOAc, 150 mmol/L MgOAc at 95°C for 35 min. The fragmented cRNA was then hybridized with a pre-equilibrated Affymetrix chip at 45°C for 14 to 16 h. After the hybridization, cocktails were removed, and the chips were then washed in a fluidic station with low-stringency buffer (6 \times saline-sodium phosphate-EDTA, 0.01% Tween 20, 0.005% antifoam) for 10 cycles (two mixes per cycle) and stringent buffer (100 mmol/L MES, 0.1 M NaCl and 0.01% Tween 20) for four cycles (15 mixes per cycle) and stained with streptavidin phycoerythrin (SAPE). This was followed by incubation with biotinylated mouse anti-avidin antibody and restained with SAPE. The chips were scanned in a HP ChipScanner (Affymetrix, Inc., Santa Clara, CA) to detect hybridization signals.

The raw scanned array images were first processed through the GCOS 3.0 (Affymetrix Corp., Santa Clara, CA) to generate probe cel intensity (*.cel) files. The *.cel files were then used to generate gene expression signal as previously described (4). We analyzed 3 normal lung samples, 4 bronchioloalveolar carcinomas, 5 samples of lung adenocarcinoma stage I, and 8 stage II adenocarcinomas of the lung.

Antibodies, cell lines, and cell culture. Dicer antibody was from Clonogene and was used at a 1:600 dilution. Proliferating cell nuclear antigen (PCNA; PC10), FXR1, PACT, and Tudor-SN antibodies were purchased from Santa Cruz Biotechnology (Santa Cruz, CA). H520 and H1568 cell lines were from the American Tissue Culture Collection (Manassas, VA). Cell lines were maintained in DMEM with 10% fetal bovine serum (Life Technologies, Sydney, Australia).

Immunoblot detection of Dicer, FXR, PACT, and Tudor-SN. The cells were washed with PBS and lysed using a cell disruption buffer (mirVANA PARIS; Ambion). The proteins were resolved by SDS-PAGE (10% polyacrylamide gel) and blotted onto a nitrocellulose membrane. The membrane was blocked with 5% powdered nonfat milk in Tris-Tween 20 buffer (pH 7.4) overnight at 4°C followed by 2 h of incubation with a 1:600 dilution of anti-Dicer antibody. PCNA, Tudor-SN, FXR1, and PACT antibodies were used as per manufacturer's protocol. The membrane was then washed three times with Tris-Tween 20 buffer and incubated with anti-mouse IgG for 1 h at room temperature. Dicer, PCNA, PACT, FXR1, and Tudor-SN expression was detected with the Super SignalWest Femto Maximum Sensitivity substrate (Pierce, Rockford, IL) according to the manufacturer's protocol.

Loss of heterozygosity studies. Loss of heterozygosity (LOH) studies were done on manually microdissected FFPE neoplastic and matched benign lung tissue as described elsewhere (11). Briefly, PCR was done on tumor and normal tissues using primers targeting short-tandem repeat units that colocalize with *Dicer* mapped to 14q32.13. The following commercial markers were used: D14S78, D14S272, D14S118, D14S267, D14S880, and D14S51 (Integrated DNA Technologies, Coralville, IA). Amplification products were detected using capillary electrophoresis (ABI 3100, Applied Biosystems, Foster City, CA). The allelic peak height ratios were calculated between normal and neoplastic samples. The sample was considered to have LOH if the allelic ratio for a specific microsatellite marker was <0.5 or >2.0.

Results

Expression of Dicer, FXR1, Tudor-SN, and PACT and histologic type of lung cancer. Normal bronchial respiratory epithelium showed diffuse cytoplasmic Dicer expression (Fig. 1A) and was used as an internal positive control. Alveolar epithelium was non-reactive for Dicer. Bronchial respiratory epithelium was used as an internal positive control. Interestingly, all nine cases of SCC on the screening tissue microarray showed high Dicer level independent of stage (Fig. 1B). This finding raised the question as to whether Dicer and other RISC proteins are differentially expressed in NSCLC lines. We compared levels of Dicer and three other RISC proteins (FXR1, Tudor-SN, and PACT) in NCI-H520 and NCI-H1568 lung cancer cell lines. Of note, NCI-H520 is derived from SCC of the lung. The NCI-I568 cell line is derived from a human lung adenocarcinoma metastatic to the lymph node. Western blot analysis of these cell lines incubated under routine cell culture conditions showed higher Dicer expression in NCI-H520 compared with NCI-H1568. Likewise, Tudor-SN, FXR1, and PACT were detected at a higher level in squamous carcinoma cell lines when compared with adenocarcinoma cells (Fig. 1C). Next, we decided to examine expression of miR-associated genes along the AAH-BAC-adenocarcinoma sequence.

Gene array analysis of miR machinery in lung adenocarcinoma. Using Affymetrix HGU133 x3p chips, we analyzed expression of all genes encoding proteins involved in miR maturation. Maturation of miR is summarized in Fig. 2A. At a false discovery rate of 5%, most nuclear components involved in miR biogenesis (*DGCR8*, *POLR2A*, and *XPO5*) showed down-regulation in BAC (*n* = 4) and stage I adenocarcinoma (*n* = 5).

Dicer showed an up to 10-fold up-regulation in stage I lung adenocarcinoma. In addition, *PACT* was up-regulated 9.4-fold in

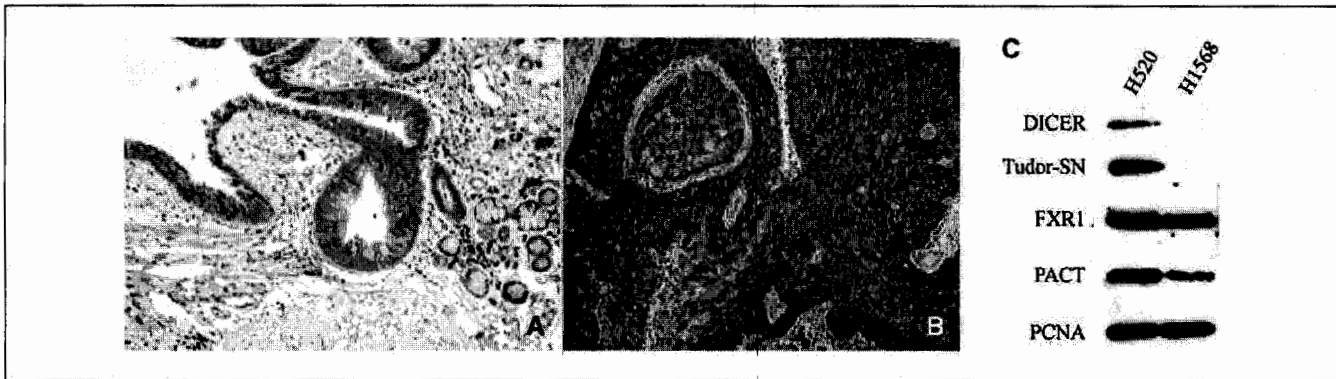


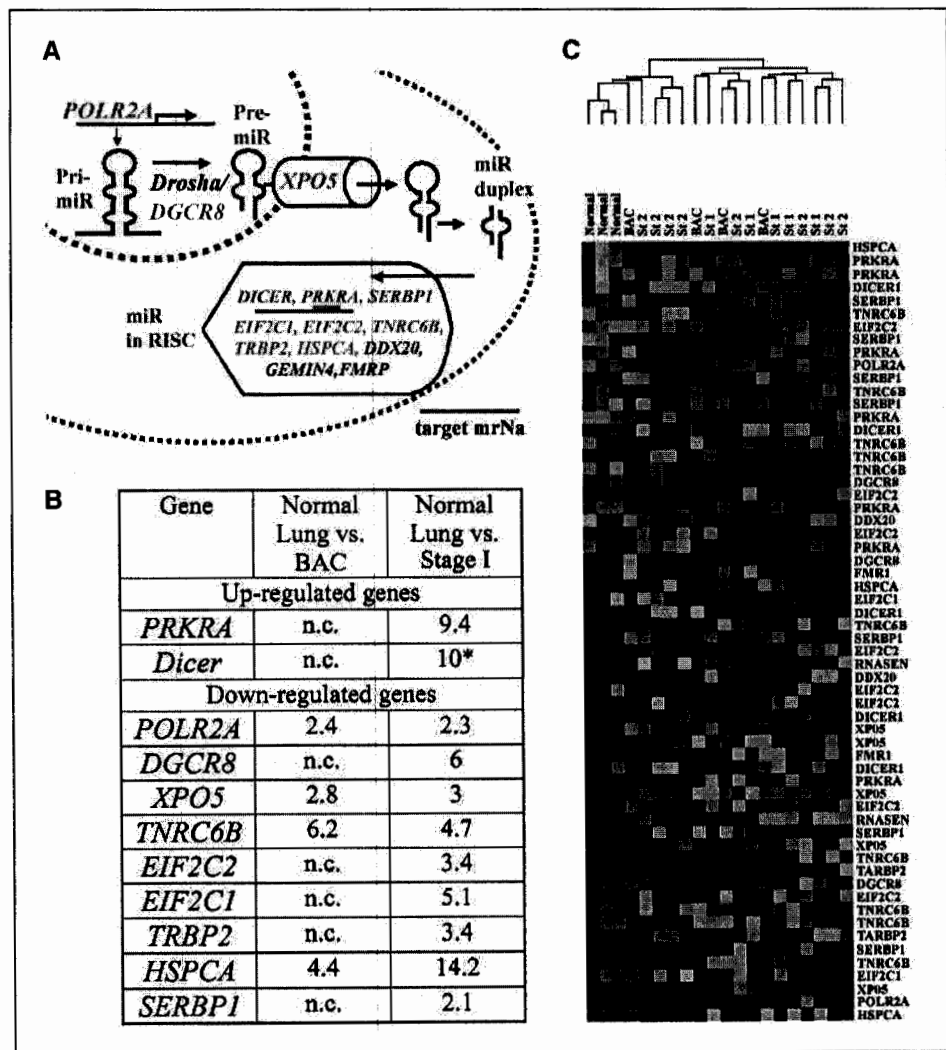
Figure 1. A, Dicer immunoreactivity in normal lung. Dicer highlights normal epithelium of the terminal bronchioli and mucus glands. Original magnification, $\times 100$ (immunohistochemistry). B, Dicer immunoreactivity in SCC of the lung. Original magnification, $\times 100$ (immunohistochemistry). C, Western blot analysis of Dicer, Tudor-SN, FXR1, and PACT expression in NCI-H520 (SCC of lung) and NCI-H1568 (metastatic adenocarcinoma of lung) cell lines. PCNA is used as a loading control.

stage I lung adenocarcinoma. Similar alterations of *PACT* in early adenocarcinomas of the lung have been previously shown (10).

Most of the other genes encoding RISC proteins were down-regulated in BAC and stage I lung adenocarcinoma. Some were

down-regulated in stage I adenocarcinoma only. For instance, *EIF2C2*, *EIF2C1*, *SERBP1*, and *TRBP2* were down-regulated 3.4-, 5.1-, 2.1-, and 3.4-fold, respectively. However, *TNRC6B* and *HSPCA* were significantly down-regulated in both BAC and stage I

Figure 2. A, schematic representation of miR maturation. Genes highlighted in green are down-regulated; genes highlighted in red are up-regulated; and genes in black showed no change. B, expression of genes encoding miR machinery in bronchioloalveolar carcinoma ($n = 4$) and stage I lung adenocarcinoma ($n = 5$), at false discovery rate of 5% (fold change). n.c., no change. C, cluster analysis in normal lung tissue, BAC, and stage I and II adenocarcinoma of the lung ($n = 8$). A dendrogram generated by a cluster analysis showing the separation of BAC and stage I lung adenocarcinoma from normal tissues on the basis of miR-associated genes differentially expressed between normal lung tissue and BAC and stage I lung adenocarcinoma. Stage II lung adenocarcinoma samples were similar to normal lung samples.



adenocarcinoma (summarized in Fig. 2B). The alteration of two additional RISC components (*MOV10* and *Tudor-SN*) was less clear due to a significant discordance in trends showed by different Affymetrix ID probes for these genes. This is usually due to the presence of uncharacterized alternatively spliced products.

Surprisingly, stage II lung adenocarcinoma samples ($n = 8$) were similar to normal lung samples (Fig. 2C).

Dicer overexpression in precursor lesions of lung adenocarcinoma: AAH and BAC. Variable *Dicer* expression along the AAH-BAC-adenocarcinoma sequence prompted us to examine the *Dicer* expression level on additional full histologic sections of AAH, BAC, and invasive adenocarcinoma. AAH was highlighted by *Dicer* expression with an average immunoreactivity score of 1.7. Fifty-five percent of all AAH cases showed *Dicer* immunoreactivity ≥ 2 (6 of 11). Even higher levels of *Dicer* were seen in BAC with the average immunoreactivity of 2.2. Eighty-three percent of BAC cases showed *Dicer* immunoreactivity ≥ 2 (14 of 17; Figs. 3 and 4). All three cases of BAC with *Dicer* immunoreactivity < 2 were of mucinous subtype.

Dicer down-regulation in invasive adenocarcinoma. When compared with BAC, invasive adenocarcinoma showed lower *Dicer* expression with the average immunoreactivity for stage I adenocarcinoma being 1.3 ($n = 23$). BAC component with higher *Dicer* level was commonly found at the periphery of the invasive adenocarcinoma. *Dicer* expression was further reduced in invasive adenocarcinomas of stage II (average *Dicer* immunoreactivity, 1.1; $n = 14$); however, the difference between *Dicer* expression in stage I and stage II adenocarcinomas was not statistically significant.

In summary, in progression from AAH through BAC to adenocarcinoma, *Dicer* is first up-regulated in AAH and BAC (Fig. 3A-C). With invasion, *Dicer* expression decreases but not to the levels seen in the normal alveolar epithelium (Fig. 3D and Fig. 4).

LOH of the *Dicer* region. Human *Dicer* is mapped to the subtelomeric region of chromosome 14 (14q32.13). The 14q32.13

locus is one of the most commonly altered loci in lung adenocarcinomas both in smokers and nonsmokers (12). Here, we show increasing LOH rates at 14q32.32 (D14S272) and 14q32.31 (D14S118). The LOH in these regions is seen in 62% of AAH (8 of 13), 66% of BAC (4 of 6), and 83% of stage II adenocarcinoma (5 of 6). However, markers mapped closer to the *Dicer* locus (D14S78 and D14S51) showed LOH only in one of six tested informative cases of BAC. None of 20 informative AAH cases and six informative cases of stages I and II adenocarcinoma showed LOH for D14S78 and D14S51.

Discussion

Normal alveolar epithelium is non-reactive for *Dicer*. Accordingly, expression analysis of adult mouse organs showed lower levels of *Dicer* mRNA in lung when compared with kidney, brain, testis, spleen, and liver (13).

In our analysis of clinical samples and representative cell lines, SCC of the lung showed higher *Dicer* expression when compared with invasive adenocarcinoma. Like *Dicer*, other RISC proteins (*FXR1*, *Tudor-SN*, and *PACT*) are present at higher levels in the SCC cell line NCI-H520 when compared with the lung adenocarcinoma cell line NCI-1568. The differential expression of RISC proteins in histologic subtypes of lung carcinoma seems to correlate with the described general trends of alterations in miR profile. Specifically, in SCC, 10 of 16 differentially expressed miRs are up-regulated, and in adenocarcinoma, 12 of 17 differentially expressed miRs are down-regulated (3).

Levels of *Dicer* dramatically increase in AAH when compared with normal alveolar epithelium. Further *Dicer* up-regulation is seen in BAC. Hence, *Dicer* overexpression might be a very early event in the development of peripheral adenocarcinomas of the lung. A decrease in *Dicer* expression seems to correlate with stromal invasion. Like *Dicer*, *PACT* is expressed strongly and diffusely in

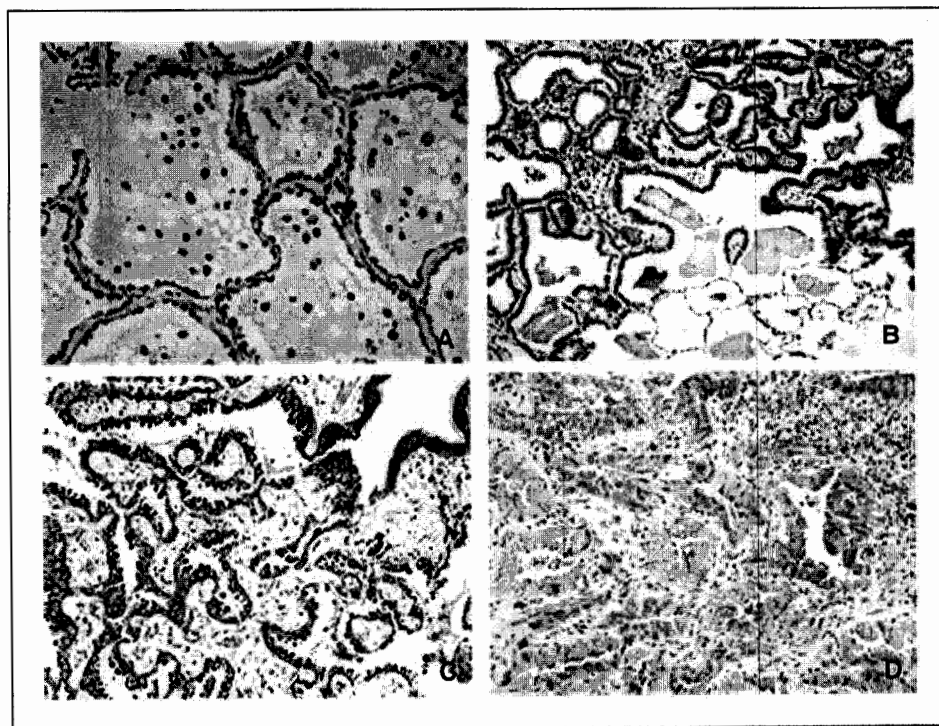


Figure 3. *Dicer* immunoreactivity in non-invasive AAH, BAC, and invasive lung adenocarcinoma. A, increased *Dicer* in AAH. Original magnification, $\times 200$ (immunohistochemistry). B and C, *Dicer* highlights BAC. Original magnification, $\times 100$ and $\times 200$, respectively (immunohistochemistry). D, *Dicer* expression in invasive adenocarcinoma, stage II. Original magnification, $\times 200$ (immunohistochemistry).

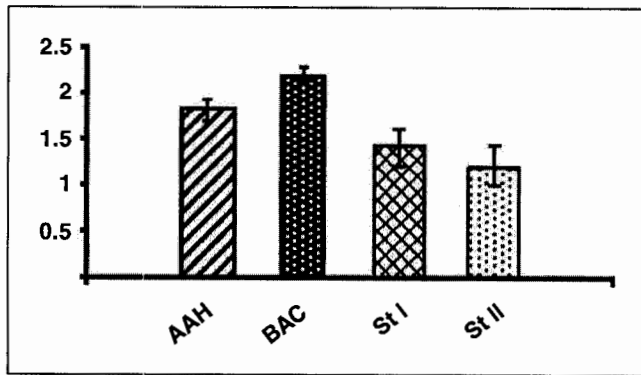


Figure 4. Schematic representation of mean Dicer immunoreactivity in pre-invasive (AAH and BAC) and invasive glandular lung neoplasia. The difference between Dicer expression in BAC and stage I (*St I*) adenocarcinoma is statistically significant ($P < 0.05$). The difference between Dicer expression in BAC and stage II (*St II*) adenocarcinoma is statistically significant ($P < 0.05$). Score 0 reflected the lack of Dicer immunoreactivity and was the most common pattern seen in benign alveolar epithelial cells.

small adenocarcinomas of the lung but not in normal alveolar epithelium (10). Similar Dicer and PACT expression is expected because it has been shown earlier that PACT may contribute to the stabilization of Dicer protein (14). The Fragile Histidine Triad, a tumor suppressor, is another protein with a similar expression pattern along the AAH-BAC-adenocarcinoma sequence (15).

We described changes in miR-associated genes and Dicer in BAC and stage I adenocarcinomas compared with normal lung tissue. The clustering analysis showed that stage II lung adenocarcinoma samples are similar to normal lung samples. Lung cancer is genetically heterogeneous with numerous secondary genetic mutations being accumulated as it progresses. In our previous LOH analysis of different microdissected areas of the same tumor, we have found tremendous i.t. heterogeneity at the loci of major tumor suppressor genes (16). This increasing heterogeneity might have precluded the detection of significant changes in levels of miR-associated genes between normal lung and stage II adenocarcinoma. However, our immunohistochemical analysis also showed lack of Dicer expression in normal alveolar epithelium and a significant decrease in Dicer expression in advanced invasive adenocarcinoma. In invasive adenocarcinoma, Dicer immunoreactivity was lower than in adenocarcinoma precursors (AAH and BAC) but still higher than in normal alveolar epithelium. Together with the undetectable level of Dicer expression in our Western Blot analysis of NCI-H1568 (a metastatic lung adenocarcinoma cell line; 30 μ g of total protein extract), these data suggest a transient up-regulation of Dicer in the earliest stages of lung adenocarcinoma. This view is further supported by an up-regulation of PACT in early adenocarcinomas (10). Wong et al. have used microsatellite probe D14S267 mapped to Mbp 94.2, ~ 400,000 bp upstream of *Dicer*, and showed 90.1% of overall heterozygosity in lung adenocarcinomas at the *Dicer* locus (12). In our specimens, the non-informative rate for this probe (D14S267) was especially high, explaining our inability to confirm the 90.1% heterozygosity at 14q32.13, the *Dicer* locus (12).

Our results are in agreement with the pioneering work by Karube Y. et al., which showed that reduced *Dicer* mRNA level is an independent adverse prognostic factor in NSCLC patients (8). Furthermore, by discovering that high Dicer expression is practically limited to prognostically favorable noninvasive bronchioloalveolar carcinoma (17), we explain how and why lower *Dicer*

expression leads to shorter postoperative survival in lung adenocarcinoma patients (8).

It is possible that altered miR machinery is still functional in BAC because only two RISC proteins (TNRC6B and HSPCA) are down-regulated. In addition, successful small interfering RNA (siRNA) experiments are reported in the BAC cell line A549 (18). It has been shown that the role of two dsRBD-containing Dicer cofactors (TRBP and PACT) may be partially redundant and differentiated to some extent. For instance, the depletion of PACT resulted in significant miR accumulation. In contrast, the depletion of TRBP has no effect on miR (14).

Little is known about the mechanisms underlying miR regulation in normal tissues and their deregulation in neoplastic processes. miR genes are commonly located at minimal regions of amplification, LOH, and breakpoint regions, suggesting that abnormal miR profiles can be caused by somatic genetic mutation (19). New details about the transcriptional and posttranscriptional regulation of miR expression have recently been discovered. When two lung cancer cell lines (A549 and NCI-H157) were treated with 5-aza-20-deoxycytidine and/or Trichostatin A, no global change in miR expression was seen, disqualifying hypermethylation and histone deacetylation as major transcriptional mechanisms controlling miR expression in lung cancer (3). However, in a separate study by Scott et al., deacetylation was thought to be an important factor capable to alter global miR levels (20).

It has been recently shown that tissue-specific mammalian miR processing can be regulated by Dicer (21). In addition, failure at the Drosha processing step explains down-regulation of miR in the P19 teratocarcinoma cell line (22).

As shown by Grimm et al. (23), short hairpin RNA (shRNA) expression in hepatocytes after i.v. infusion resulted in fatal dose-dependent liver injury. Adverse effects were most likely caused by competition of exogenous siRNA pathway with the endogenous miR pathway and saturation of Exportin-5 and one or more other components of miR machinery (23). The status of Dicer and other proteins of the miR machinery in various histologic subtypes of lung cancer and different stages of lung carcinogenesis might explain abnormalities in the miR profile of NSCLC and may help predict the toxicity of and susceptibility to future RNAi-based therapy. With the development of RNAi-based treatments, it might be crucial to learn how the changes of RISC described here affect each branch of the small RNA pathway (endogenous miR pathway and experimental, exogenous, siRNA pathway) and what modality of RNAi delivery (e.g., chemically modified siRNA versus shRNA from viral or non-viral vectors) will be most promising in a specific cancer type. Further studies are needed to predict the effect of decreased *Exportin-5* and lower levels of RISC proteins in adenocarcinoma of the lung shown here on susceptibility to RNAi-based therapy and rates of RNAi-induced adverse effects.

Acknowledgments

Received 9/25/2006; revised 11/11/2006; accepted 12/11/2006.

Grant support: Postdoctoral Pathology Research Training Program (RT-00147 and CC-99FUND) from the Department of Pathology, University of Pittsburgh Medical Center (S. Chiosea); American Cancer Society Research Scholar grant RSG-05-246-01-GMC (R.W. Sobol); Susan G. Komen Breast Cancer Foundation grant BCTR0403276 (R.W. Sobol); University of Pittsburgh Medical Center Health System Competitive Medical Research Fund (R.W. Sobol); University of Pittsburgh Cancer Institute (R.W. Sobol); National Cancer Institute grant R01 CA098249 (J.H. Luo).

The costs of publication of this article were defrayed in part by the payment of page charges. This article must therefore be hereby marked *advertisement* in accordance with 18 U.S.C. Section 1734 solely to indicate this fact.

We thank Raja Seethala, MD and Julia Kofler, MD for review of the article and helpful critiques.

References

1. Devesa SS, Bray F, Vizcaino AP, Parkin DM. International lung cancer trends by histologic type: male:female differences diminishing and adenocarcinoma rates rising. *Int J Cancer* 2005;117:294-9.
2. Kerr KM. Pulmonary preinvasive neoplasia. *J Clin Pathol* 2001;54:257-71.
3. Yanaihara N, Caplen N, Bowman E, et al. Unique microRNA molecular profiles in lung cancer diagnosis and prognosis. *Cancer Cell* 2006;9:189-98.
4. Chiosea S, Jelezcova E, Chandran U, et al. Up-regulation of Dicer, a component of the microRNA machinery, in prostate adenocarcinoma. *Am J Pathol* 2006;169:1812-20.
5. Hammond SM. MicroRNAs as oncogenes. *Curr Opin Genet Dev* 2006;16:4-9.
6. Calin GA, Croce CM. MicroRNA-cancer connection: the beginning of a new tale. *Cancer Res* 2006;66:7390-4.
7. Carmichael JB, Provost P, Ekwall K, Hobman TC. ago1 and dcr1, two core components of the RNA interference pathway, functionally diverge from rdp1 in regulating cell cycle events in *Schizosaccharomyces pombe*. *Mol Biol Cell* 2004;15:1425-35.
8. Karube Y, Tanaka H, Osada H, et al. Reduced expression of Dicer associated with poor prognosis in lung cancer patients. *Cancer Sci* 2005;96:111-5.
9. Harris KS, Zhang Z, McManus MT, Harfe BD, Sun X. Dicer function is essential for lung epithelium morphogenesis. *Proc Natl Acad Sci U S A* 2006;103:2208-13.
10. Roh MS, Kwak JY, Kim SJ, et al. Expression of double-stranded RNA-activated protein kinase in small-size peripheral adenocarcinoma of the lung. *Pathol Int* 2005; 55:688-93.
11. Esposito NN, Hunt JL, Bakker A, Jones MW. Analysis of allelic loss as an adjuvant tool in evaluation of malignancy in uterine smooth muscle tumors. *Am J Surg Pathol* 2006;30:97-103.
12. Wong MP, Lam WK, Wang E, Chiu SW, Lam CL, Chung LP. Primary adenocarcinomas of the lung in nonsmokers show a distinct pattern of allelic imbalance. *Cancer Res* 2002;62:4464-8.
13. Nicholson RH, Nicholson AW. Molecular characterization of a mouse cDNA encoding Dicer, a ribonuclease III ortholog involved in RNA interference. *Mamm Genome* 2002;13:67-73.
14. Lee Y, Hur I, Park SY, Kim YK, Suh MR, Kim VN. The role of PACT in the RNA silencing pathway. *EMBO J* 2006;25:522-32.
15. Kerr KM, MacKenzie SJ, Ramasami S, et al. Expression of Fhit, cell adhesion molecules and matrix metalloproteinases in atypical adenomatous hyperplasia and pulmonary adenocarcinoma. *J Pathol* 2004;203:638-44.
16. Dacic S, Ionescu DN, Finkelstein S, Yousem SA. Patterns of allelic loss of synchronous adenocarcinomas of the lung. *Am J Surg Pathol* 2005;29:897-902.
17. Yokose T, Suzuki K, Nagai K, Nishiwaki Y, Sasaki S, Ochiai A. Favorable and unfavorable morphological prognostic factors in peripheral adenocarcinoma of the lung 3 cm or less in diameter. *Lung Cancer* 2000; 29:179-88.
18. Halder SK, Anumanthan G, Maddula R, et al. Oncogenic function of a novel WD-domain protein, STRAP, in human carcinogenesis. *Cancer Res* 2006;66: 6156-66.
19. Zhang L, Huang J, Yang N, et al. microRNAs exhibit high frequency genomic alterations in human cancer. *Proc Natl Acad Sci U S A* 2006;103:9136-41.
20. Scott GK, Mattie MD, Berger CE, Benz SC, Benz CC. Rapid alteration of microRNA levels by histone deacetylase inhibition. *Cancer Res* 2006;66:1277-81.
21. Obernosterer G, Leuschner PJ, Alenius M, Martinez J. Post-transcriptional regulation of microRNA expression. *RNA* 2006;7:1161-7.
22. Thomson JM, Newman M, Parker JS, Morin-Kensicki EM, Wright T, Hammond SM. Extensive post-transcriptional regulation of microRNAs and its implications for cancer. *Genes Dev* 2006;20:2202-7.
23. Grimm D, Stretz KL, Jopling CL, et al. Fatality in mice due to oversaturation of cellular microRNA/short hairpin RNA pathways. *Nature* 2006;441:537-41.